

COMPUTATIONAL STUDY OF THE KURAMOTO-SIVASHINSKY EQUATION

YIORGOS S. SMYRLIS * AND DEMETRIOS T. PAPAGEORGIOU †

Abstract. We report the results of extensive numerical experiments on the Kuramoto-Sivashinsky equation in the strongly chaotic regime as the viscosity parameter is decreased and increasingly more linearly unstable modes enter the dynamics. General initial conditions are used and evolving states do not assume odd-parity. A large number of numerical experiments are employed in order to obtain quantitative characteristics of the dynamics. A classification of most strongly attractors is given based on numerical solutions and several data processing tools.

1. Introduction. The Kuramoto-Sivashinsky equation is one of the simplest one-dimensional PDE's which exhibits complex dynamical behavior. As an evolution equation it arises in a number of applications including concentration waves and plasma physics ([3], [17], [18], [19]), flame propagation and reaction diffusion combustion dynamics ([27], [28]), free surface film-flows ([2], [12], [26]) and two-phase flows in cylindrical or plane geometries [6], [9], [22], [31], [32].

If the system has length L , the equation can be normalized to 2π -periodic domains and reads

$$(1) \quad \begin{aligned} u_t + uu_x + u_{xx} + \nu u_{xxxx} &= 0, \\ (x, t) &\in \mathbb{R}^1 \times \mathbb{R}^+, \\ u(x, t) &= u(x + 2\pi, t), \end{aligned}$$

where $\nu = \frac{\pi^2}{L^2} > 0$ represents a dimensionless wavelength of u . The limit $\nu \rightarrow 0$ corresponds to the waves in (1) becoming infinitely long. Linearization of (1) about the zero state shows that the first $\text{mod}(\nu^{-\frac{1}{2}})$ Fourier modes are unstable and grow exponentially. It is well-known, from numerical experiments for instance (see below), that solutions to (1) become increasingly irregular as ν is decreased.

An analytical study of the KS equation was carried out by Nicolaenko et al. [21] (referred to as [NST]), where it is shown that if the initial data are in L^2 and are of odd-parity then the solutions remain in L^2 for all time and there is a globally attracting set also bounded in L^2 . The bound depends on the value of L or ν and [21] gives the estimate

$$(2) \quad \limsup_{t \rightarrow \infty} \|u(\cdot, t)\|_2 \leq \text{const} \cdot \nu^{-3/2}.$$

The odd-parity restriction of [21] has been removed recently by several authors. Goodman [11] considers general smooth initial data and obtains a bound of the same form as (2). This bound is improved further, however, by Il'yashenko [15] and independently using a more classical approach by Collet et al. [4], and is

$$(3) \quad \limsup_{t \rightarrow \infty} \|u(\cdot, t)\|_2 \leq \text{const} \cdot \nu^{-13/10}.$$

* Department of Mathematics and Statistics, University of Cyprus, Nicosia, Cyprus. The work of Y.S. Smyrlis was supported by NATO Grant CRG 920097.

† Department of Mathematics and Center for Applied Mathematics and Statistics, New Jersey Institute of Technology, Newark NJ 07102. The work of D.T. Papageorgiou was supported by the National Science Foundation Grant NSF-DMS-9003227 and by NATO Grant CRG 920097.

Note that the analysis in [4] and [15] applies also to odd-parity initial conditions and so is an improvement of the method in [NST]. For recent results on the analyticity of the solution see Collet et al. [5].

A lot of numerical work preceded the theoretical studies and revealed many interesting nonlinear phenomena including complex dynamics and chaotic trajectories as the dissipation parameter ν decreases. Earlier works include the computations of Cohen et al. [3], Sivashinsky and Michelson [29], Aimar [1], and Manneville [20]. Systematic explorations of phase space were carried out by Hyman and Nicolaenko [13] and Hyman et al. [14], Papageorgiou and Smyrlis [24], [30] and Coward et al. [6] who report on many features of the dynamics. Kevrekidis et al. [16] computed the bifurcation diagram for relatively large values of ν , using a bifurcation algorithm. For smaller values of ν unsteady phenomena set in; it was first found by Papageorgiou and Smyrlis [24] and also Smyrlis and Papageorgiou [30], that in the case of odd-parity initial conditions there is a period-doubling route to chaos. Extensive numerical solutions were employed to provide strong evidence that the route to chaos is according to the Feigenbaum scenario ([7], [8]); in addition the universal constants computed by Feigenbaum for one-dimensional nonlinear non-invertible maps, were computed from our numerical data with two digit accuracy. In the sequel we term chaotic dynamics just beyond the accumulation point, in parameter space, as Feigenbaum chaos.

In this article we present the results of extensive numerical computations for general initial conditions. Comparisons with previous studies (e.g. [13], [14], [16]) have been made where there is an overlap with full agreement. Our particular interest is in lower values of ν where the dynamics gets increasingly complicated.

2. Numerical Methods. Guided by the theoretical results we find that a traditional Fourier Galerkin scheme is very suitable for the computations, when modified appropriately to take care of stiffness problems for large wavenumbers. (The scheme is presented and discussed elsewhere, [25].)

We have carried out a very large number of numerical experiments, testing more than 800 values of the dissipation parameter ν ranging from¹ $\nu = .99999999$ to $\nu = .002$. For representative values of ν , several runs were carried out to ensure that the behavior of the attractor does not change with more Fourier coefficients or finer time step. The size of the truncation ranged from $N = 4$ to $N = 512$ making computation in the latter case rather slow. In addition, many cases had to be followed for very long times in order to achieve convergence to the corresponding attractor and/or to accurately classify the attractor. For example in the case $\nu = .1212267996068$, the attractor is periodic with 2^{14} distinct maxima and as many minima in the L^2 norm as a function of time. This particular value of ν follows previous ones corresponding

¹ If $\nu \geq 1$ then

$$(4) \quad \lim_{t \rightarrow +\infty} u(x, t) = \bar{u}_0 = \frac{1}{2\pi} \int_0^{2\pi} u_0(x) dx,$$

since KS equation implies that

$$\frac{1}{2} \frac{d}{dt} |u(\cdot, t)|_2^2 = |u_x(\cdot, t)|_2^2 - \nu |u_{xx}(\cdot, t)|_2^2$$

and for $u \in L^2[0, 2\pi]$, 2π -periodic, with $\int_0^{2\pi} u(x) dx = 0$ we have the following inequalities:

$$|u|_2 \leq |u_x|_2 \leq |u_{xx}|_2$$

On the other hand if $\nu \leq 0$ the problem is ill-posed.

to 13 period doubling bifurcations. The period is estimated to be $T \approx 25573$, which corresponds to approximately 5.1×10^7 time steps and each step corresponding to substeps. Satisfactory convergence to the periodic attractor occurred after 10^9 time steps.

Classification of the nature of the attractors at different ν , made it possible to determine the windows in parameter space. The majority of the computational effort was spent in the accurate determination of the limits of ν -windows, and in addition to determine whether transition between two kinds of attractors was smooth or not. A case of a smooth transition is a bifurcation; examples are period-doublings and eigenvalue bifurcations of the Jacobian of the flux of the dynamical system - these cause transition from stationary/traveling attractors to periodic or chaotic ones. An example of a non-smooth transition is the coexistence of two or more invariant locally attracting sets in a subinterval $[\nu_1, \nu_2]$. It is found, for instance, that while one attracts *most* of the initial data, as ν varies, the second one becomes suddenly more likely to attract most initial data. For example, in the case of $\nu = .232$, we have coexistence of a unimodal traveling attractor and of one with periodically appearing homoclinic bursts. The second one is *more attracting*. Even though the exact bifurcation values of ν depend on the accuracy of the numerical scheme, the nature of the bifurcation does not depend on the accuracy provided that the method is of sufficient accuracy since the system has finite degrees of freedom. This observation requires the use of higher accuracy when we seek better approximation of the bifurcation values of ν .

Some of the data processing tools used are briefly described next. Periodic attractors are evaluated from the energy versus time plot - $E(t) = |u(t, \cdot)|_{L^2}$ and the corresponding more convincing once we obtain the energy phase plane - i.e. $E(t)$ versus $dE(t)/dt$, where the values of $dE(t)/dt$ are accurately obtainable using a suitable interpolation of several points $(t_k, E(t_k))$. Periodic attractors correspond to closed phase curves and the number of minima/maxima is the number of the points where the phase curves intersect the E -axis, i.e. $dE(t)/dt = 0$ with $d^2E(t)/dt^2 > 0$ or < 0 respectively. More accurate quantitative data such as the exact period and the exact values of the local extrema are needed in order to accurately determine period doubling bifurcations and study the potential fractal nature of the return map² of the extrema. Such accuracy was achieved by calculation of the extrema by an optimized polynomial interpolation over a sufficiently large number of points $(t_k, E(t_k))$. The polynomial of the interpolation is obtained by a suitably weighted least squares method over consecutive points, many more than the degree of the polynomial sought for. Weights in the least squares approximation, reduce the effects of higher order polynomial terms and the round-off error caused by the computation of the quantity used in the interpolation. Weights are introduced to make the points which are closer to the local extremum have a higher contribution to the interpolation. The original motivation in developing the interpolation algorithm is in the accurate determination of period doubling bifurcations and the appearance of the Feigenbaum universal constants. (See Smyrlis and Papageorgiou [30].) This method turned out to be extremely helpful in determining features such as the fractal nature of attractors, by detecting such behavior in the return map of the energy minima, for example. Most successfully it has enabled us to detect and classify quasiperiodic attractors. In certain cases the return map plot has fractal nature and foliations are observable when one plots

² Let $a_n, n \in \mathbb{N}$ be a sequence of real numbers, then the set of points $(a_n, a_{n+1}), n \in \mathbb{N}$, which is a subset of \mathbb{R}^2 , is called the *Return Map* of $(a_n)_{n \in \mathbb{N}}$. In the case of a function $f : [0, \infty] \rightarrow \mathbb{R}$ the return map of f is the return map of the sequence of the local minima (or maxima or extrema) of f .

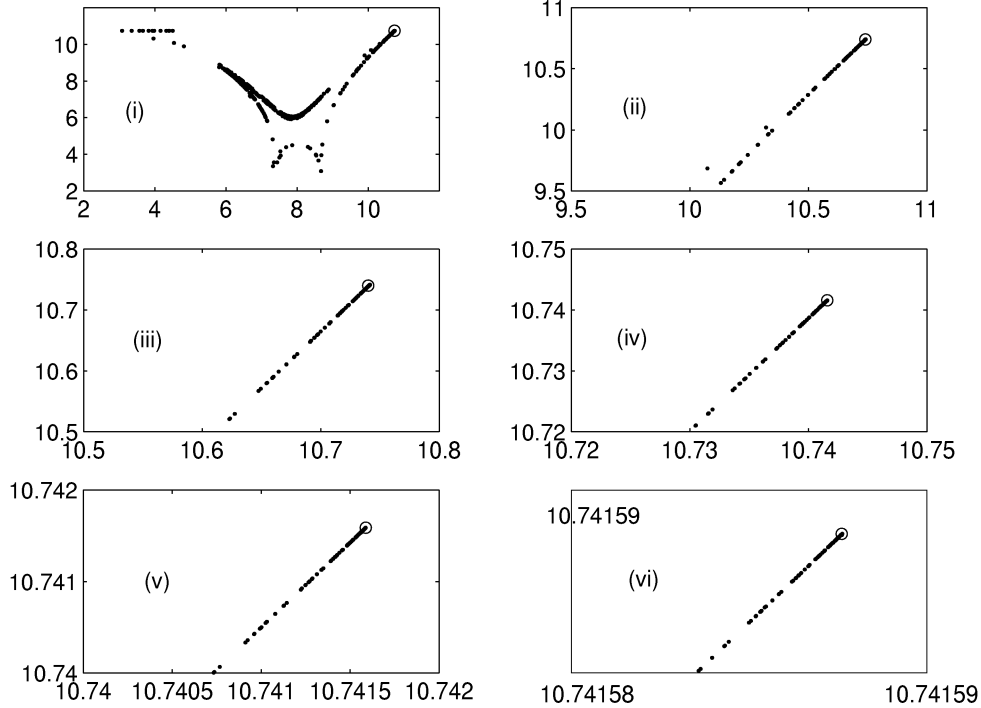


FIG. 1. Return map of energy minima at $\nu = 0.12115$ depicting the self-similarity of the attractor. (ii)-(vi) are successive magnifications of (i) in the neighborhood of the open circle. An overall magnification factor of 10^5 is shown.

successive magnifications of the graphs. An example of such a construction is given in Figure 1 which corresponds to a $\nu = 0.12115$ and is in a region of chaotic homoclinic bursts just beyond the Feigenbaum period-doubling cascade. Self-similarity of the attractor is supported by the return map; successive enlargements are made in the neighborhood of the open circle and an enlargement of order 10^5 takes place in going from (i) to (vi). The need for an accurate determination of critical points is crucial in achieving such magnifications - absence of accuracy would produce noisy data sets with little hope of exhibiting self-similarity.

3. Numerical Results. For values of ν larger than about 0.1 a fairly complete picture of the dynamics has been given by numerous authors ([13], [14], [16]) Steady state or traveling waves, including their bifurcation diagrams are computable by well-developed bifurcation algorithms, see for example ([16]). Our interest is on the spatio-temporal evolution in chaotic attractors which led to the development of the accurate code, tracking the time evolution of solutions, described in Section 2. Some interesting windows in this range are (i) periodic homoclinic bursts, (ii) a period-doubling route to chaos, (iii) chaotic homoclinic bursts. The period-doubling cascade has been confirmed to follow the Feigenbaum scenario and the Feigenbaum constants have been calculated from our data.

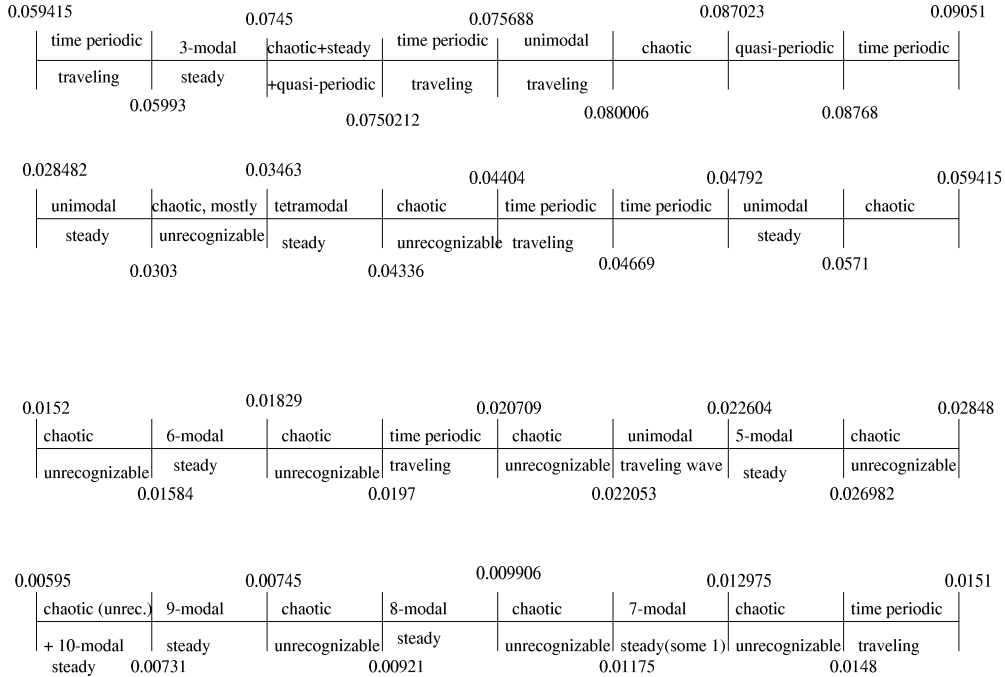


FIG. 2. Schematic of computed attractors at lower values of ν .

3.1. Dynamics for lower values of ν : $\nu < 0.09$. As ν decreases the dynamics become more complicated. A larger number of determining modes is required and co-existence of attractors is more likely. From a numerical viewpoint the computations become more expensive and accuracy criteria more stringent. A large number of numerical experiments has been carried out over several years and a summary of the attractors is given in Figure 2. The Figure represents the ν -line (not drawn to scale) along with various attractors found by us; note that the given attractors are not necessarily global ones but their window boundaries delineate regions where stability is lost. The type of attractor was determined by applying the data analysis described earlier.

It can be seen from the Figure that the dynamics is quit complex but can be classified using the methods described earlier. Of particular interest is a route to chaos via a quasi-periodic attractor as seen in the first three windows of the figure. A time periodic attractor loses stability to a quasi-periodic one at $\nu = 0.087679$ and there is transition to chaos below $\nu = 0.087023$. Quasi-periodicity was determined by studying the return map.

Another feature of the solutions is that among the regions of different unsteady and complicated spatio-temporal motions there emerge stable fixed point attractors with increasingly higher modal behavior, i.e. with shorter periods. It has been verified that these stable (but not global) states, are obtainable from the following similarity property of the equation (see [10]): Given an integer N , if $u(x; \nu)$ is a solution then so is $Nu(Nx; \nu/N^2)$. In other words we can start with one of the global unimodal

steady states with $\nu > .3$, approximately, and apply the transformation with different N to generate steady state solutions at lower geometrically decreasing values of ν . Not all such solutions are stable, but the ones found by our computations are. It has also been found that computed stable states emerge from application of the similarity transformation to global attractors near $\nu = 0.6$. This is an interesting result since it is in line with modulational stability studies of steady states as N becomes large (see [10], [23]). Full details of these feature are given elsewhere ([25]).

4. Conclusions. We have given many quantitative features of solutions of the Kuramoto-Sivashinsky equations computed with general initial data and spatially periodic boundary conditions. Features such as strange attractors and periodic or chaotic bursting phenomena have been elucidated. Of particular interest is a set of computed multimodal solutions found at decreasing values of ν and supported on smaller and smaller windows. It has been shown that these solutions (the last computed one is a decamodal profile, i.e. one with all Fourier coefficients zero except those which are multiples of 10) derive from the unimodal fixed point attractor in $.3 < \nu < 1$, by a self-similar transformation property of the equation. It can be concluded that such solutions are at least linearly stable (in the sense that they are computable as large time solutions of a nonlinear initial value problem) and our numerical results are in full agreement with the stability theory of Frisch et al [10] and the modulation theory of Papageorgiou et al [23] who study the stability of such multimodal steady states. The numerical results given here provide strong support for the modulation stability theories.

REFERENCES

- [1] Aimar, E.T., *Étude numérique d'une équation d'évolution nonlinéaire dérivant instabilité thermodynamique d'un front de flamme*, Thèse, Troisième cycle, Université de Provence (1982).
- [2] Benney, D.J., *Long Waves in Liquid films*, J. Math. and Phys. **45** (1966), pp. 150-155.
- [3] Cohen, B.I., Krommes, J.A., Tang, W.M., Rosenbluth, M.N., *Non-linear saturation of the dissipative trapped ion mode by mode coupling*, Nucl. Fusion, **16**, (1976), pp. 971-992.
- [4] Collet, P., Eckmann, J.-P., Epstein, H., Stubbe, J., *A global attracting set for the Kuramoto-Sivashinsky equation*, Commun. Math. Phys., **152** (1993), pp. 203-214.
- [5] Collet, P., Eckmann, J.-P., Epstein, H., Stubbe, J., *Analyticity for the Kuramoto-Sivashinsky equation*, Physica D, **67** (1993), pp. 321-326.
- [6] Coward, A.V., Papageorgiou, D.T., Smyrlis, Y.S., *Nonlinear stability of oscillatory core-annular flow: A generalized Kuramoto-Sivashinsky equation with time periodic coefficients*, Zeit. Angew. Math. Phys. (ZAMP), **46** (1995), pp. 1-39.
- [7] Feigenbaum, M., *The onset of spectrum turbulence*, Phys. Lett. B, **74** (1979), pp. 375-378.
- [8] Feigenbaum, M., *The transition to aperiodic behavior in turbulent systems*, Commun. Math. Phys., **77** (1980), pp. 65-86.
- [9] Frenkel, A.L., Babchin, A.J., Levich, B.G., Shlang, T., Sivashinsky, G.I., *J. Colloid. Interface Sci.*, **115** (1987), pp. 225.
- [10] Frisch, U., She, Z.S., Thual, O., *Viscoelastic behavior of cellular solutions of the Kuramoto-Sivashinsky equation*, J. Fluid Mech., **168** (1986), pp. 221-240.
- [11] Goodman, J., *Stability of the Kuramoto-Sivashinsky equation and related systems*, Comm. Pure Appl. Math., **XLVII** (1994), pp. 293-306.
- [12] Hooper, A.P., Grimshaw, R., *Nonlinear instability at the interface between two fluids*, Phys. Fluids, **28** (1985), pp. 37-45.
- [13] Hyman, J.M., Nicolaenko, B., *The Kuramoto-Sivashinsky equations, a bridge between PDEs and dynamical systems*, Physica D, **18** (1986), pp. 113-126.
- [14] Hyman, J.M., Nicolaenko, B., Zaleski, S., *Order and complexity in the Kuramoto-Sivashinsky model of turbulent interfaces*, Physica D, **23** (1986), pp. 265-292.
- [15] Il'yashenko, J.S., *Global analysis of the phase portrait for the Kuramoto-Sivashinsky equation*, J. Dyn. Diff. Equations, **4**(4) (1992), pp. 585-615.

- [16] Kevrekidis, I.G., Nicolaenko, B., Scovel, C., *Back in the saddle again: a computer assisted study of the Kuramoto-Sivashinsky equation*, SIAM J. Appl. Math., **50** (1990), pp. 760-790.
- [17] Kuramoto, Y., *Diffusion induced chaos in reactions systems*, Progr. Theoret. Phys. Suppl., **64** (1978), pp. 346-367.
- [18] Kuramoto, Y., Tsuzuki, T., *On the formation of dissipative structures in reaction diffusion systems*, Progr. Theoret. Phys., **54** (1975), pp. 687-699.
- [19] Kuramoto, Y., Tsuzuki, T., *Persistent propagation of concentration waves in dissipative media far from thermal equilibrium*, Progr. Theoret. Phys., **55** (1976), pp. 356-369.
- [20] Manneville, P., *Lyapunov exponents for the Kuramoto-Sivashinsky equations*, Proc. Conf. on Turbulence, Nice 1984, Lecture Notes in Physics, Springer-Verlag, New York (1985).
- [21] Nicolaenko, B., Scheurer, B., Temam, R., *Some global dynamical properties of the Kuramoto-Sivashinsky equations: Nonlinear stability and attractors*, Physica D, **16** (1985), pp. 155-183.
- [22] Papageorgiou, D.T., Maldarelli, C., Rumschitzki, D.S., *Nonlinear interfacial stability of core-annular film flow*, Phys. Fluids A, **2**, No. 3 (1990), pp. 340-352.
- [23] Papageorgiou, D.T., Papanicolaou, G.C., Smyrlis, Y.S., *Modulational stability of periodic solutions of the Kuramoto-Sivashinsky equation*, ICASE Report No. 93-44 and SIAM J. Applied Math., submitted.
- [24] Papageorgiou, D.T., Smyrlis, Y.S. *The route to chaos for the Kuramoto-Sivashinsky equation*, Theoret. Comput. Fluid Dynamics, **3** (1991), pp. 15-42.
- [25] Papageorgiou, D.T., Smyrlis, Y.S. *Computational study of ordered and chaotic solutions of the Kuramoto-Sivashinsky equation*, ICASE Report, and to be submitted to Physica D.
- [26] Shlang, T., Sivashinsky, G.I., *Irregular flow of a liquid film down a vertical column*, J. Phys., **43**, (1982), pp. 459-466.
- [27] Sivashinsky, G.I., *Nonlinear analysis of hydrodynamic instability in laminar flames, Part I. Derivation of basic equations*, Acta Astronautica, **4** (1977), pp. 1176-1206.
- [28] Sivashinsky, G.I., *On flame propagation under conditions of stoichiometry*, SIAM J. Appl. Math., **39** (1980), pp. 67-82.
- [29] Sivashinsky, G.I., Michelson, D.M., *On irregular wavy flow of a liquid down a vertical plane*, Prog. Theor. Phys. **63** (1980) 2112-2114.
- [30] Smyrlis, Y.S., Papageorgiou, D.T., *Predicting chaos for infinite-dimensional dynamical systems: The Kuramoto-Sivashinsky equation, a case study*, Proc. Nat. Acad. Sci. USA, **88** No. 24 (1991), pp. 11129-11132.
- [31] Tilley, B.S., Davis, S.H. and Bankoff, S.G. *Linear stability theory of two-layer flow in an inclined channel*, Phys. Fluids, **6** (1994), pp. 3906-3922.
- [32] Tilley, B.S., Davis, S.H. and Bankoff, S.G. *Nonlinear long-wave stability of superposed fluids in an inclined channel*, J. Fluid Mech., **277** (1994), pp. 55-83.